

10 Particle Physics at LHC/CMS

C. Amsler, R. Kaufmann, H. Pruyss, C. Regenfus, P. Riedler and S. Steiner

in collaboration with:

ETH-Zürich, Paul Scherrer Institut (PSI), Universität Basel and 143 institutes from 30 other countries

CMS Collaboration

The detection of heavy flavors at LHC demands an excellent reconstruction capability for secondary vertices in the high rate environment close to the primary interaction point. The innermost tracking will be provided by a three layer cylindrical pixel barrel detector. We are responsible for the design, test and purchase of the pixel sensors, for the mechanical support structure and for the cooling system.

10.1 Lorentz-angle in irradiated silicon

In 1999 we proceeded with the analysis of the pixel test runs performed at the CERN SPS with 225 GeV/c pions (see last year's annual report and ref. [1]). The depletion thickness of two silicon pixel detectors (8×32 pixels of size $125 \times 125 \mu\text{m}^2$) was measured using the grazing angle method, in which incident particles impinge at small angles α (of typically 7°) with respect to the sensor surface (fig.10.1). This angle was measured accurately for each incident particle by our high precision silicon telescope [1]. The depletion thickness was determined from the "street length" i.e. the number of hit pixels along the beam direction. One of the detectors had been irradiated at PSI with 6×10^{14} pions per cm^2 and annealed for more than one year in a cooled environment of 2°C . For the non-irradiated detector the full depletion thickness of $280 \mu\text{m}$ could be reached, while for the irradiated device we achieved a reduced depletion thickness of $160 \mu\text{m}$.

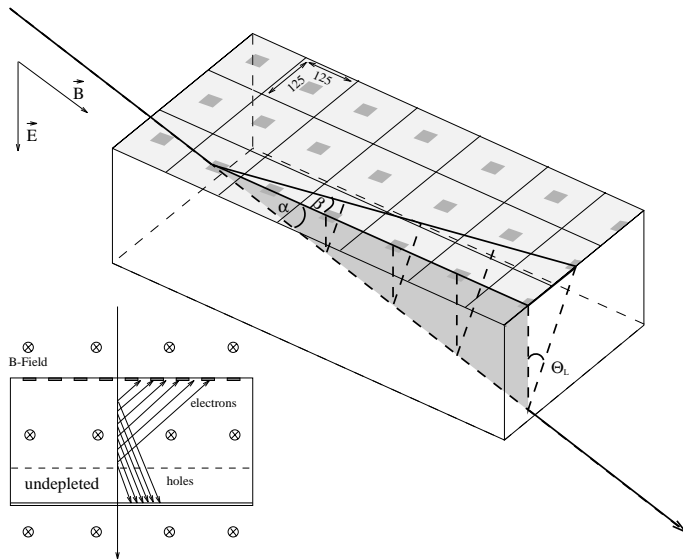


Figure 10.1: *Three dimensional sketch of the pixel detector traversed by a charged particle under the grazing angle α . The Lorentz angle is denoted by Θ_L . The front view of the detector on the left shows the drift directions of electrons and holes.*

The apparatus was immersed in a magnetic field parallel to the beam axis, provided by two Helmholtz coils. Due to deflection in the magnetic field the charge carriers did not move along the electric field lines but drifted at an angle Θ_L (the Lorentz angle) towards the adjacent pixel row (fig. 10.1). The energy deposit was therefore shared among adjacent pixels. By comparing the charge deposits we were able to determine the Lorentz angle: $\Theta_L = (18.2$

$\pm 1.2^\circ$) at 3 Tesla for the non-irradiated detector. The charge sharing between pixels will lead to a position resolution at CMS of typically $15\mu\text{m}$ (r.m.s), well below the individual pixel dimensions.

For the irradiated detector, however, the situation turns out to be more complex. Thanks to the tracking provided by our telescope we could observe a peculiar behaviour as a function of depth. The Lorentz angle appears to vary with the depth of the migrating electron cloud. Figure 10.2(left) shows how the energy deposit is shared between two adjacent pixel rows for the non-irradiated detector. As expected, charge sharing is nearly linear as a function of depth. It increases with depth due to the longer drift distance to the sensors. This is not the case for the irradiated device (right) for which charge sharing increases more rapidly with depth. This different behaviour must be attributed to the changes that occurred after irradiation (type inversion, increase in effective doping concentration and charge trapping from irradiation defects). The effect is not fully understood yet. It leads to a smaller Lorentz angle of about 6° at 3 Tesla just below the sensors and to a larger angle of about 27° at larger depths [2].

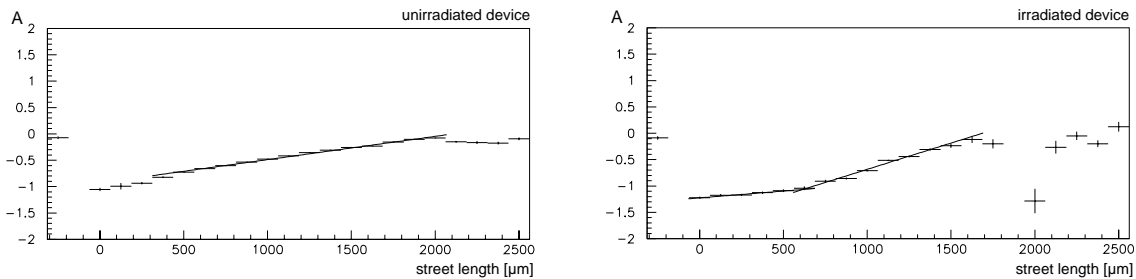


Figure 10.2: *Asymmetry $A = (Q_n - Q_i)/(Q_n + Q_i)$ between charges collected by adjacent pixels as a function of pixel street length (hence depth) for the non-irradiated (left) and the irradiated detector (right). Q_i refers to the charge collected by pixels just above the particle track and Q_n to the charge collected by the next adjacent pixel row (left or right, depending on the sign of the magnetic field).*

10.2 Sensor developments

The barrel detector is made of three cylindrical layers, 53 cm long with radii of 4, 7 and 11 cm, the first layer being used only during initial low luminosity runs [3]. Each layer is made of two half-cylinders to allow insertion into the CMS detector. A pixel unit cell contains 53×52 pixels. The dimensions of the (square) pixels have been increased from $125\mu\text{m}$ in the original proposal to $150\mu\text{m}$. Two rows of 8 cells build a module and a row of 8 modules builds a facet of length 53 cm and width 1.75 cm. The total number of pixels to be read out is about 3×10^7 .

The bulk material is n -type (thickness of $300\mu\text{m}$) and the pixel implants are n^+ (larger concentration of donors). A p^+ layer is deposited on the opposite side of the wafer to form the junction. In the original (non-irradiated) detector the depletion layer grows with applied bias voltage in the the n -bulk from the p^+ side. During irradiation type inversion occurs and the depletion layer then grows from the pixels side.

The n^+ sensors are manufactured by ion implantation. A thin layer of SiO_2 is then generated in a O_2 vapour environment at 1000°C , after which a small square hole is etched at the center of the pixel to provide the electrical contact. The sensor is covered with a thin layer of aluminium which also flows into the contact hole, see fig. 10.4 (right) below. After passivation a small hole is etched in the SiO_2 layer in the corner of the sensors and the

aluminium is covered with a titanium-tungsten alloy and gold (underbump metallization). This provides the contact with the readout chip through the indium bump. Figure 10.3 (right) shows an electronic microscope photograph of a readout chip designed at PSI, and the indium bumps.

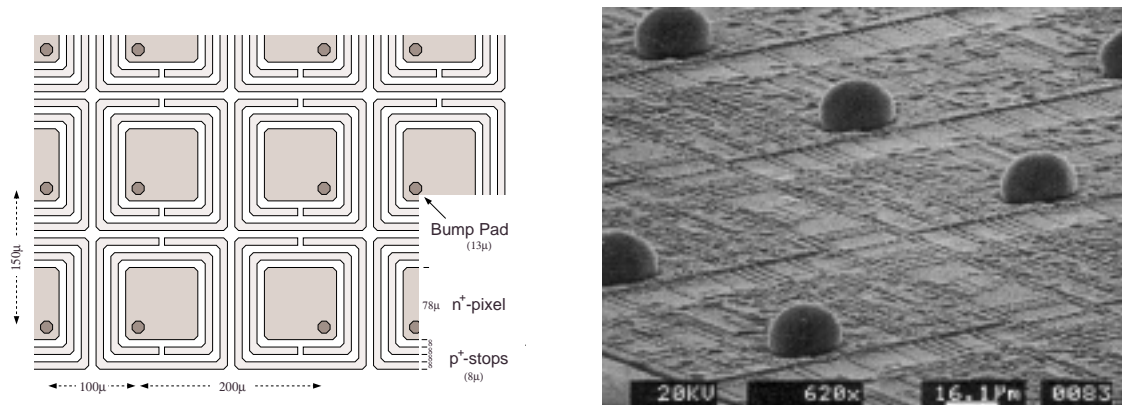


Figure 10.3: *sensors with threefold guard ring structure. Right: Radiation hard readout chip showing the indium bumps.*

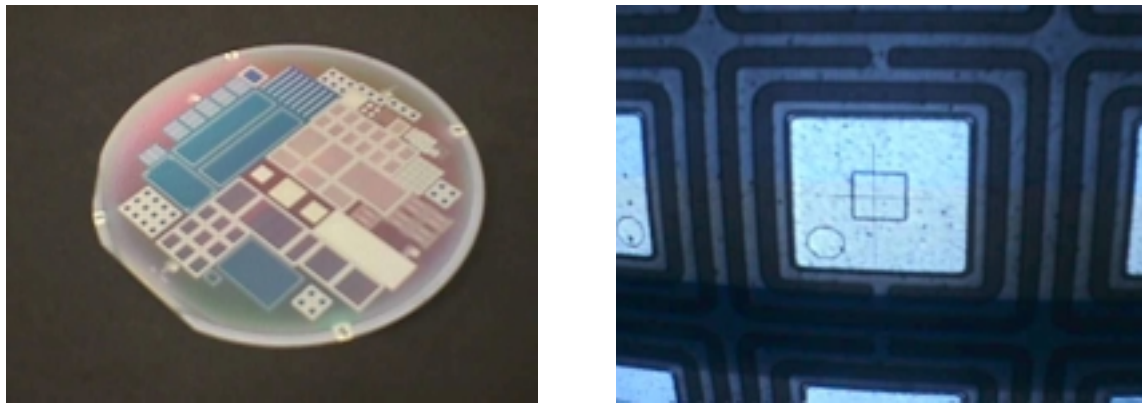


Figure 10.4: *Left: One of the 4" wafers delivered by CSEM. Right: Microscope photograph of one of the sensors showing the p^+ -stop rings (dark) and the metallic layer (bright area) showing the small square and round contact holes for the electrical connections to the n^+ implant and the indium bump, respectively. The faint crosshairs stem from the digital camera.*

One expects that a small fraction of the pixels might have poor electrical connections with the readout chip through the indium bumps. The accumulation of charge would then lead to local breakdown. We have designed a maze around every sensor to increase the resistance between pixels (fig. 10.3, left). The atolls (p^+ -stop rings) provide a high resistive path between the pixels and prevent the charging up, whenever the bump bond fails. A pixel is thus a square of $78 \mu\text{m}^2$ surrounded by two p^+ -stop rings, $8 \mu\text{m}$ wide with a separation pitch of $8 \mu\text{m}$.

We have designed the masks and ordered prototypes for the pixels sensors. A batch of 24 wafers (4"), some with high (5-6 $\text{k}\Omega \text{ cm}$) and some with low (1-2 $\text{k}\Omega \text{ cm}$) resistivity were ordered from CSEM in Neuchâtel. Since oxygen impurities have been found to improve the radiation hardness of silicon detectors [4], we have ordered an additional batch of oxygenated wafers which have not been delivered yet. Figure 10.4 shows a photograph of one of the

delivered wafers which contains various pixel and atoll geometries. (Our sensor submission also included silicon pads to be used on PSI/SLS projects.) We have performed mechanical stress tests and also electrical tests of the (so far not irradiated) prototypes by measuring the capacitances C on a probe station. The depletion thickness d grows as the square root of the bias voltage while C increases with $1/d$. Therefore $1/C^2$ should increase linearly with bias voltage, as observed, until full depletion is achieved (Fig. 10.5, left). Figure 10.5 (right) shows the current between a pixel at 0.2 V and its grounded neighbours as a function of bias voltage. After full depletion, reached at a bias voltage of 160 V (kink), a resistance of a few $M\Omega$ is achieved. The residual current is due to e^- accumulation under the oxide layer.

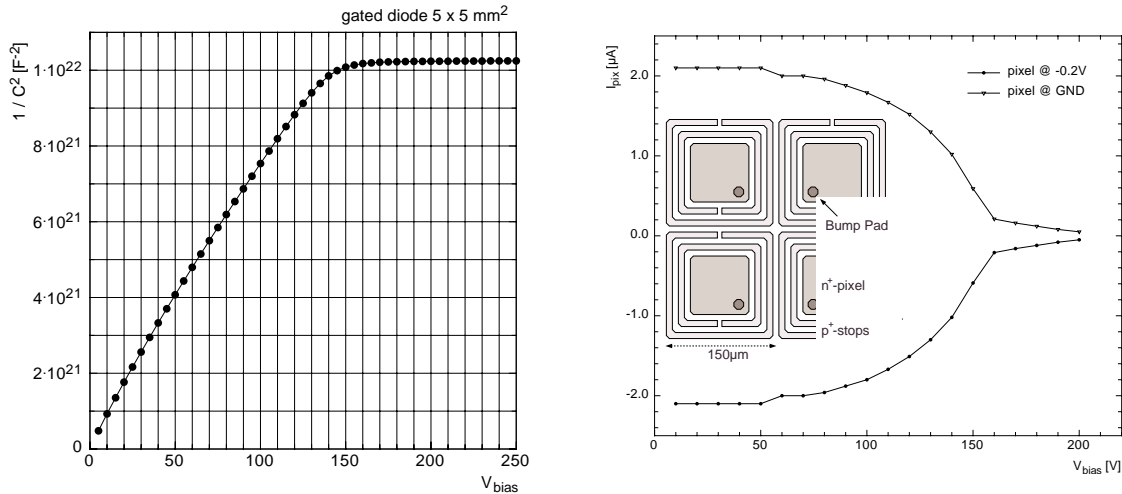


Figure 10.5: *Left: Measurement on a probe station of the capacitance as a function of bias voltage. The maximum depletion thickness is achieved in the plateau region. Right: Interpixel current as a function of bias voltage. Full depletion is reached at 160 V (kink).*

However, the resistivity will change after radiation damage. This will be investigated next summer. The delivered sensors will be cut and bump-bonded to the DMILL PSI30 readout chips developed at PSI. After irradiation at the CERN-PS we will perform tests of the atoll structure (breakdown performance, charge collection efficiency between pixels) using our tracking telescope. The R&D phase of the project will continue until 2002 and will be followed by the mass production phase. LHC will be commissioned in 2005 at which time we should have delivered the two innermost pixel layers for the initial low luminosity runs.

References

- [1] M. Glättli, Diplomarbeit, Universität Zürich (1998).
- [2] R. Kaufmann and B. Henrich, Proc. of the ENDEASD Workshop, Santorin (1999) and Nucl. Instr. and Methods in Phys. Research A (in print).
- [3] Technical Design Report of the CMS Tracker, CERN/LHCC 98-6 (1998)
- [4] M. Moll, E. Fretwurst, G. Lindström (ROSE Collaboration), Nucl. Instr. Meth. in Phys. Res. A 439 (2000) 282.